

**Helium in superstrong magnetic fields**

O.-A. Al-Hujaj and P. Schmelcher

*Theoretische Chemie, Institut für Physikalische Chemie der Universität Heidelberg, INF 229, 69120 Heidelberg, Germany*

(Received 20 December 2001; revised manuscript received 4 November 2002; published 26 February 2003)

We investigate the helium atom embedded in a superstrong magnetic field  $\gamma=100\text{--}10000$  a.u. All effects due to the finite nuclear mass for vanishing pseudomomentum are taken into account. The influence and the magnitude of the different finite mass effects are analyzed and discussed. Full configuration interaction calculations are performed for singlet and triplet states for the magnetic quantum numbers  $M=0, -1, -2, -3$ , as well as positive and negative  $z$  parities. Up to six excited states for each symmetry are studied. With increasing field strength the number of bound states decreases rapidly and we remain with a comparatively small number of bound states for  $\gamma=10^4$  a.u. within the symmetries investigated here.

DOI: 10.1103/PhysRevA.67.023403

PACS number(s): 32.60.+i, 32.30.-r, 32.10.-f

**I. INTRODUCTION**

The term “strong” field characterizes a situation for which an interacting particle system exposed to a field is in the nonperturbative regime, i.e., where the magnetic forces are of the same order of magnitude or greater than the Coulomb binding force. For the ground state of the hydrogen atom this corresponds to field strengths  $\gamma \geq 1$  a.u. (1 a.u. corresponds to  $2.35 \times 10^5$  T). We refer to the term “superstrong” to indicate a field strength of 100 a.u. and more.

The motivation to study atoms and molecules in strong magnetic fields originates from several sources. Certainly the properties of these systems are interesting from a pure theoretical point of view. Due to the competition of the spherically symmetric Coulomb potential and the cylindrically symmetric magnetic-field interaction we encounter a non-separable, nonintegrable problem already for a one-electron system, i.e., the hydrogen atom. Therefore, it is necessary to develop new techniques to solve the Schrödinger equation in strong magnetic fields. The discovery of strong magnetic fields on the surface of magnetic white dwarfs ( $10^2\text{--}10^5$  T) and neutron stars ( $10^5\text{--}10^9$  T) is a further major motivation. The spectra of these astrophysical objects are mainly influenced by the presence of magnetic fields. For the analysis of atmospheres of magnetic white dwarfs and neutron stars, it is very important to have reliable data on the behavior of matter in strong magnetic fields. As an example, we mention the white dwarf GrW+70°8247. The interpretation of its spectrum was a key to our understanding of the properties of spectra of magnetic white dwarfs, in general (see Refs. [1–5]).

Highly accurate data are available for hydrogen in strong magnetic fields since many years (see, e.g., [6,7]). This system is now understood to a very high degree. Beyond hydrogen there is significant interest in accurate data on heavier elements such as He, Na, Fe, and even molecules. Especially helium plays an important role in the atmosphere of certain magnetic white dwarfs (see, e.g., [8–10]). There were several attempts to calculate accurate energies for bound states of helium, the requirements for astrophysical applications being a relative accuracy of  $\approx 10^{-4}$  for the two-particle binding energies for a large number of states. We will concentrate here on investigations that address the high-field regime. In

1975 Mueller *et al.* [11] calculated the few lowest levels of He for  $\gamma$  up to 20 000 a.u. using a variational approach. Virtamo [12] presented Hartree-Fock calculations on the ground state (which is a triplet state with magnetic quantum number equal to  $-1$ ). The same state has been considered by Pröschl [13] in 1982 in the range 21–21000 a.u. Vincke and Baye [14] provide correlated calculations ( $\gamma=4.2, 42$ , and 420 a.u.) for the lowest singlet and triplet states with positive  $z$  parity and magnetic quantum numbers  $M=0, -1, -2$ . In the work of Thurner [15], several triplet states are considered in the very broad range  $\gamma=8 \times 10^{-4}\text{--}8 \times 10^3$  a.u. We mention also the important work by Becken and Schmelcher [16–19], which covers many symmetries and a large number of excited states for the range  $\gamma=8 \times 10^{-4}\text{--}100$  a.u.

The properties of matter in superstrong magnetic fields are especially interesting for the physics of cooling neutron stars [20–22]. In this field regime, finite nuclear mass effects become increasingly important. This is due to the fact, that the corresponding energy shifts are of the order of  $\gamma/M_0$ , where  $M_0$  is the mass of the nucleus. Indeed  $\gamma/M_0$  becomes for superstrong magnetic fields of the same order of magnitude as the ionization energies. Of course, the conceptual and, in particular, the computational situation becomes more complex when the full Hamiltonian, i.e., the Hamiltonian for finite nuclear mass, is addressed. For both neutral [23,24] as well as charged systems [23–32], we encounter additional couplings among the different electrons as well as couplings between the collective and electronic motion.

Some approximations to account for finite nuclear mass effects in the case of ions are available: An approximate separation of the collective and relative motion of the charged system has been introduced in Ref. [25] and applied to calculate the finite nuclear mass corrections for low-lying levels of hydrogenic ions in a magnetic field [26]. Elaborated multi configuration Hartree-Fock computations as well as adiabatic approximations were given in Ref. [32] for  $\text{He}^+$ . The behavior and properties of the  $\text{He}^+$  ion are crucial to determine the one-particle ionization energies  $I^{(\text{He})}$  for helium. However, the results of Ref. [32] are due to the adiabatic approximation, not accurate enough to reliably evaluate, together with the corresponding results of He, the quantities  $I^{(\text{He})}$  (see below).

In the present paper, we provide a full configuration interaction (CI) calculation for helium in superstrong magnetic fields. All finite mass effects at zero pseudomomentum are taken into account and are analyzed. In Sec. II, we will describe the Hamiltonian, and some technical details concerning our calculation. Furthermore, we provide some remarks on the problem of the threshold energies. In Sec. III, we analyze the differences of the Hamiltonian in the infinite nuclear mass frame from the exact Hamiltonian. Ionization energies and transition wavelengths are provided in Sec. IV.

## II. FORMULATION OF THE PROBLEM

### A. Hamiltonian and symmetries

To investigate the He atom, we apply a nonrelativistic approach. This is well justified by the fact that relativistic corrections have been shown to be very small in strong and even superstrong magnetic fields [33,34]. For the sake of simplicity, we take the electronic-spin  $g$  factor to be 2, but our results can be easily adapted to any  $g$  factor by multiplying the spin operators and their eigenvalues by  $g/2$ . On the other hand, the ionization energies and transition wavelengths, which are presented in this paper are not affected by this choice. The magnetic-field vector, which is chosen to point in the  $z$  direction, will be denoted by  $\mathbf{B}$ , whereas its magnitude is  $\gamma=|\mathbf{B}|$ .

The first step in our approach is the pseudoseparation of the collective and relative motion for the Hamiltonian in the laboratory frame, which exploits the conservation of the so-called pseudomomentum  $\mathbf{K}$  [23,24,35,36]. The resulting transformed Hamiltonian is divided into three parts, which are denoted by  $H_1$ ,  $H_2$ , and  $H_3$ . The operator  $H_1 = \mathbf{K}^2/(2M_A)$  involves only center-of-mass (c.m.) degrees of freedom, where  $M_A$  is the mass of the atom.  $H_3$  contains exclusively electronic degrees of freedom. The operator  $H_2 = -(1/M_A)(\mathbf{B} \times \mathbf{K}) \cdot \sum_i \mathbf{r}_i$  represents the coupling between  $H_1$  and  $H_3$ , i.e., between the c.m. and electronic degrees of freedom. It involves the motional electric field  $(1/M_A)(\mathbf{B} \times \mathbf{K})$ , which arises due to the motion of the (neutral) atom in the magnetic field and is oriented perpendicular to the magnetic field. This coupling is proportional to the pseudomomentum, and therefore, vanishes for vanishing pseudomomentum. The pseudoseparation is possible for neutral systems only, since only then all components of the pseudomomentum commute.

Within the present work, we assume a vanishing pseudomomentum. This assumption is, in general, justified, i.e., a good approximation for an atom at rest or small velocity. As a result, we have no additional motional electric field and we are left with the electronic Hamiltonian  $H_3$ , which in the following will be denoted as  $H(M_0, \gamma)$ , where  $M_0$  is the mass of the nucleus. In atomic units it takes the following form (internal coordinates are taken with respect to the nucleus):

$$H_3 = H(M_0, \gamma) = H_{\text{rm}} + H_{\text{mp}}, \quad (2.1)$$

where

$$H_{\text{rm}} = \sum_{i=1}^2 \left( \frac{1}{2\mu} p_i^2 + \frac{1}{2\mu'} \mathbf{B} \cdot \mathbf{l}_i + \frac{1}{8\mu} (\mathbf{B} \times \mathbf{r}_i)^2 - \frac{2}{|\mathbf{r}_i|} + \mathbf{B} \cdot \mathbf{s}_i \right) \quad (2.2)$$

$$+ \frac{1}{|\mathbf{r}_1 - \mathbf{r}_2|} \quad (2.3)$$

and

$$H_{\text{mp}} = \frac{1}{2M_0} \sum_{i \neq j} \left( \mathbf{p}_i \cdot \mathbf{p}_j - \mathbf{p}_i \cdot (\mathbf{B} \times \mathbf{r}_j) + \frac{(\mathbf{B} \times \mathbf{r}_i) \cdot (\mathbf{B} \times \mathbf{r}_j)}{4} \right). \quad (2.4)$$

The reduced masses are  $\mu = 1/(1 + 1/M_0)$  and  $\mu' = 1/(1 - 1/M_0)$ . The Hamiltonian consists of three parts. The first part contains the one-particle operators  $(1/2\mu)p_i^2$ , the Zeeman terms  $(1/2\mu')\mathbf{B} \cdot \mathbf{l}_i$ , the diamagnetic terms  $(1/8\mu)(\mathbf{B} \times \mathbf{r}_i)^2$ , the attractive Coulomb interaction with the nucleus  $-2/|\mathbf{r}_i|$ , and the spin Zeeman terms  $\mathbf{B} \cdot \mathbf{s}_i$ . The second part contains the two-particle operator (2.3), which describes the repulsive Coulomb interaction between the two electrons. The third operator is the so-called mass polarization operator  $H_{\text{mp}}$ . It arises due to the transformation from the laboratory frame to the internal coordinates, which are taken relative to the nucleus. The reader should note that the Hamiltonian (2.1) has the same good quantum numbers as the Hamiltonian for infinite nuclear mass: the total spin  $S^2$ , the component  $S_z$  of the total spin, the magnetic quantum number  $M$ , and the total spatial  $z$  parity  $\Pi_z$  (parity is not an independent symmetry, it can be deduced from the mentioned symmetry operations). In the following, we will denote the states by  $\nu^{2S+1}M^{\Pi_z}$ , where  $2S+1$  is the spin multiplicity and  $\nu = 1, 2, 3 \dots$  denotes the degree of excitation within a given symmetry subspace.

If we compare  $H(M_0, \gamma)$  in Eq. (2.1) to the electronic Hamiltonian of helium in the infinite nuclear mass frame [16]  $H(\infty, \gamma)$ , we observe two different kinds of corrections due to the finite nuclear mass. First, we encounter reduced masses  $\mu$  and  $\mu'$  in  $H_{\text{rm}}$  which provide the so-called normal mass corrections. The spectrum of the Hamiltonian  $H_{\text{rm}}$  which contains exclusively these normal mass corrections can be related to the spectrum of the Hamiltonian  $H(\infty, \gamma')$  at a different field strength  $\gamma'$ , via a unitarian transformation and an additional trivial energy shift (see Sec. III and also Refs. [6,16,37]). The second type of finite nuclear mass effects is due to the mass polarization operators  $H_{\text{mp}}$ . We will call these specific finite mass corrections. They are by no means trivial and are related to the correlation of the electrons (the corresponding operators contain one-particle operators of both electrons). If the electrons behave in a correlated way, the specific nuclear mass effects can be enhanced.

### B. Technical remarks

Some comments concerning our computational approach are in order. Its basic ingredient is an anisotropic Gaussian basis set, which was put forward by Schmelter and Cederbaum [38]. This one-particle basis is sufficiently flexible to describe finite electronic systems for any field strength and

was successfully applied to several atoms and molecules in magnetic fields [16–19,39–42].

In the case of atoms, all matrix element can be calculated analytically and evaluated efficiently [16,17]. The price, which has to be paid, is that for each field strength and each symmetry, the basis set has to be (nonlinearly) optimized: We search for a set of basis functions, which provides within a finite computational strategy the lowest possible energies for the corresponding one-particle problems (H, He<sup>+</sup>, etc). This is a standard procedure in atomic and molecular physics, since the direct nonlinear optimization of many particle wave functions, using many configurations, is not feasible. In order to ensure convergence of the one-particle problem, we compare the obtained binding energies to the accurately known data for the one-particle problem in a strong magnetic field [6,7]. To investigate the helium atom, we select sets of anisotropic Gaussian basis functions, which yield relative accuracies for the binding energies of the one-particle problems of the order of  $10^{-7}$  to  $10^{-9}$  for the ground states, and  $10^{-4}$  to  $10^{-6}$  for the higher excited states of each symmetry. The relative accuracies of the binding energies do not depend on the magnetic-field strength, although the total-energy increases approximately linearly. This is due to the anisotropic (Gaussian-like) form of the one-particle basis functions, which describes the free electrons in the magnetic field (Landau states) exactly and, therefore, also the linear rise of the kinetic energy. One intelligent guess for the starting points of the nonlinear optimization are parameter sets that optimally solve the same problem at a nearby magnetic-field strength. Particularly, we developed optimization algorithms and corresponding tools, which allow an almost automatic construction of a basis set. A one-particle basis set typically consists of 200–400 basis functions that yield 3000 to 5000 two-particle configurations. Many aspects for the selection of basis functions for helium in intermediate and strong magnetic fields have been extensively discussed in Ref. [16]. The full CI approach leads then to a generalized eigenvalue problem. Numerical problems arise in this generalized eigenvalue problem if near linear dependencies exist in the basis set. These dependencies cannot fully be avoided, but the resulting numerical instabilities can be removed by a cutoff of the small eigenvalues of the corresponding overlap matrix. This approach is a standard one in the literature for the generalized eigenvalue problem and has shown its applicability especially for helium at zero and nonzero magnetic-field strength [16–19]. A comparison to previously published data (in particular, for the field-free case) demonstrates the degree of convergence, which can be obtained within this method. Convergence of the full problem is checked by observing the two-particle binding energies as a function of the number of orthogonal configurations. As an example, we demonstrate convergence for the two-particle binding energies of the helium atom in the  $^10^+$  symmetry subspace at  $\gamma=100$  a.u. in Fig. 1.

The procedure, consuming the most part of CPU time in the above approach, is the evaluation of the electron-electron matrix elements. Although analytical formulas for all matrix elements are available, it is important to have efficient algorithms for their evaluation, since the matrix elements for the

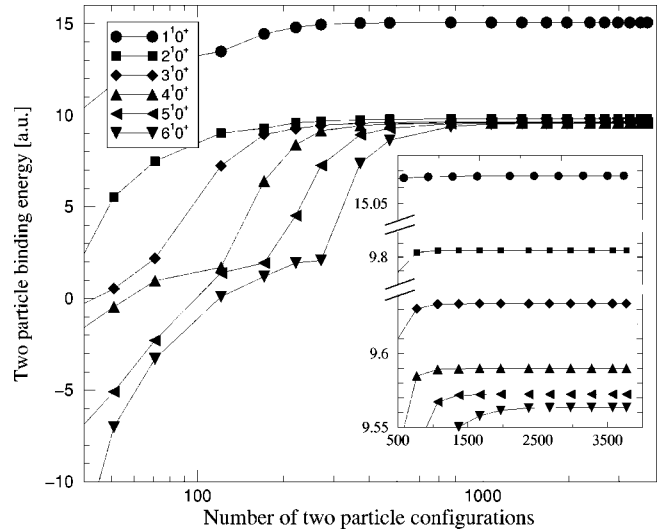


FIG. 1. Two-particle binding energies in atomic units for helium embedded in a magnetic field  $\gamma=100$  a.u. for the states with  $^10^+$  symmetry as a function of the number of two-particle configurations. The inset shows an enlargement for large numbers of configurations.

electron-electron Coulomb interaction are by no means trivial. A detailed and sophisticated analysis of their analytical representation is crucial. In the simplest form, it contains multiple sums of hypergeometric functions [16,17]. For the evaluation of the hypergeometric function all possible analytical continuation formulas have been worked out (see Ref. [43]) and this made it possible to reduce the time for the calculation of the matrix elements by a factor of 50 compared to a straightforward implementation. We emphasize that the present investigation would have been impossible without these efforts.

### C. Threshold

Solving the generalized eigenvalue problem yields the total energies of the atom. These energies are, however, not of primary interest: they increase almost linearly with the field strength due to the rise of the kinetic energy in the presence of the field. The relevant energies are, e.g., the transition and ionization energies which are, in the high-field regime addressed here, by several orders of magnitude smaller than the total energies and, therefore, the common linear increase of energy has to be subtracted. Similar to the one-electron problem (see arguments above), the relative accuracy of the two-particle binding energies is not affected by the rise of the total energies. To obtain the one-particle ionization energies, we need, however, to know the ground-state energy of the He<sup>+</sup> ion in the magnetic field *taking into account the finite nuclear mass*. But unlike the case of infinite nuclear mass, where the appropriate levels can be calculated from the corresponding energies of the hydrogen atom (see, e.g., Ref. [7]) via scaling relations (see, for example, Ref. [6]), these energies are unknown: Accurate investigations on He<sup>+</sup> including the unique coupling between the collective and electronic motion have not been performed. This coupling inherently mixes the collective and electronic motion and the exact

ground state, therefore, includes both. Only qualitative results [32] for the energies of the moving  $\text{He}^+$  ion in a superstrong magnetic field are known. As a result our uncertainty for the one-particle binding energies of He are much larger than for the two-particle binding energies. The reader should note that using just the threshold energy of  $\text{He}^+ + e^-$  for fixed nucleus  $E_{\text{fm}}^{\text{th}}$  provides a wrong description for the ionization energies of helium in superstrong fields.

The Hamiltonian for the  $\text{He}^+$  ion reads in atomic units as follows:

$$H_{\text{He}^+} = H_a + H_b + H_c, \quad (2.5)$$

$$H_a = \frac{1}{2(M_0+1)} \left( \mathbf{P} - \frac{1}{2} \mathbf{B} \times \mathbf{R} \right)^2, \quad (2.6)$$

$$H_b = \frac{M_0+2}{(M_0+1)^2} \left( \mathbf{P} - \frac{1}{2} \mathbf{B} \times \mathbf{R} \right) \cdot (\mathbf{B} \times \mathbf{r}), \quad (2.7)$$

$$H_c = \frac{1}{2\mu} \mathbf{p}^2 + \frac{1}{2} \left( \omega_1 - \frac{\omega_2}{M_0} \right) \mathbf{B} \cdot \mathbf{l} + \frac{1}{8} \left( \omega_1^2 + \frac{\omega_2^2}{M_0} \right) (\mathbf{B} \times \mathbf{r})^2. \quad (2.8)$$

Here,  $H_a$  describes the collective motion of the ion as a free particle with charge 1 and mass  $M_0+1$  moving in a magnetic field ( $\mathbf{R}$  and  $\mathbf{P}$  are the center-of-mass coordinate and momentum, respectively). The operator  $H_b$  couples the electronic and collective motion. The operator  $H_c$  is the electronic part of the  $\text{He}^+$  Hamiltonian with  $\omega_1 = 1 + 1/(M_0+1)^2$  and  $\omega_2 = 1 + (2M_0+1)/(M_0+1)^2$ .

Although the exact energy threshold for  $\text{He} \rightarrow \text{He}^+ + e^-$  is not available, some approximations to it can be concluded. One of these approximations, namely,  $E_{\text{zpmc}}^{\text{th}}$  (the index zpmc stands for zero-point mass-corrected) ignores the coupling  $H_b$  between the collective and electronic motion. The corresponding values of the energy threshold consist of the sum of the eigenenergies of the electronic Hamiltonian  $H_c$  and the zero-point energy belonging to  $H_a$ . This zero-point energy for the collective motion is the energy for the lowest Landau state.  $E_{\text{zpmc}}^{\text{th}}$  is typically too high, i.e., the ionization energies are overestimated, since the coupling  $H_b$ , which is neglected in this approximation, tends to reduce the threshold energy. All ionization energies shown in the present work are calculated by applying  $E_{\text{zpmc}}^{\text{th}}$ .

A second approximation to the energy threshold ignores both the zero-point energy of the ion and the coupling term, i.e.,  $H_a$  and  $H_b$ . Therefore, only the eigenenergies of the mass-corrected electronic Hamiltonian  $H_c$  are taken into account. This threshold is denoted as  $E_{\text{mc}}^{\text{th}}$ . It is motivated by the fact, that for an infinitely strong magnetic field the energetic contributions due to the zero-point energy of  $H_a$  and the coupling  $H_b$  exactly cancel. A third alternative threshold energy  $E_{\text{ad}}^{\text{th}}$  is obtained by employing the adiabatic expansion approach presented in Ref. [32]. Since this approximation only takes into account the lowest Landau energy for the c.m. motion, it becomes increasingly accurate for increasing energetic separation between the Landau levels (and, therefore, increasing magnetic-field strength). For field strengths

below 2000 a.u., however, this approximation is not reliable. It can be observed, that the threshold energy  $E_{\text{ad}}^{\text{th}}$  approaches the threshold energy  $E_{\text{mc}}^{\text{th}}$  in the limit of high fields.

### III. FINITE NUCLEAR MASS EFFECTS

There is a transformation, which connects the spectrum of the infinite nuclear mass Hamiltonian  $H(\infty, \gamma)$  with the spectrum of the Hamiltonian  $H_{\text{rm}}$  [16]. This transformation reads as follows:

$$U H_{\text{rm}} U^{-1} = \mu H \left( \infty, \frac{\gamma}{\mu^2} \right) - \frac{\gamma}{M_0} \sum_i (l_{z_i} + s_{z_i}). \quad (3.1)$$

Here,  $U$  denotes a unitarian transformation, which transforms  $\mathbf{r} \rightarrow \mathbf{r}/\mu$  and  $\mathbf{p} \rightarrow \mathbf{p}\mu$ . The second term on the right-hand side of Eq. (3.1) represents a field dependent trivial energy shift, since the total  $z$  component of the spin and of the orbital angular momentum are conserved quantities, respectively.

From Eq. (3.1) it can be seen, that the leading mass correction to the energy is of the order of  $\gamma/M_0$ . For the states with magnetic quantum number  $M < 0$ , this correction is positive, which means that the corresponding energies are shifted linearly with  $\gamma$  and eventually pass the ionization threshold. The corresponding bound electronic states are therefore ionized. This energetical shift depends exclusively on  $M$ ,  $S_z$ ,  $\gamma$ , and the nuclear mass  $M_0$ .

The energy difference  $\Delta E_{\text{rm}} = E_{\text{rm}}(\gamma) - E(\infty, \gamma)$ , where  $E_{\text{rm}}$  denote the eigenvalues of  $H_{\text{rm}}$  and  $E(\infty, \gamma)$  those of  $H(\infty, \gamma)$ , can be related to the energy difference  $\Delta E_{\text{rm}}^e$  of the lowest eigenvalues of the Hamiltonian  $H_f^e$  and  $H_{\text{rm}}^e$  (see below) of a specific symmetry. The operator  $H_f^e$  describes two free noninteracting electrons

$$H_f^e = \sum_{i=1}^2 \frac{1}{2} \mathbf{p}_i^2 + \frac{\gamma}{2} l_{z_i} + \frac{\gamma^2}{8} \rho_i^2, \quad (3.2)$$

whereas  $H_{\text{rm}}^e$  refers to the corresponding ‘‘artificial’’ Hamiltonian with reduced masses

$$H_{\text{rm}}^e = \sum_{i=1}^2 \frac{1}{2\mu} \mathbf{p}_i^2 + \frac{\gamma}{2\mu} l_{z_i} + \frac{\gamma^2}{8\mu} \rho_i^2. \quad (3.3)$$

For the energetically lowest Landau level with negative magnetic quantum number  $M$  and vanishing momentum in  $z$  direction, we have

$$\Delta E_{\text{rm}}^e = \frac{\gamma}{M_0} (1 + |M|). \quad (3.4)$$

It cannot be expected, that the normal mass corrections of the helium atom  $\Delta E_{\text{rm}}$  follow exactly Eq. (3.4), because the Hamiltonian  $H_{\text{rm}}$  contains the interaction between the two electrons and of the electrons with the nucleus. However, it is suggestive to introduce a parameter  $\delta(\gamma)$  such that

$$\Delta E_{\text{rm}} = E_{\text{rm}}(\gamma) - E(\infty, \gamma) = \Delta E_{\text{rm}}^e(\gamma) \{1 + \delta(\gamma)\}.$$

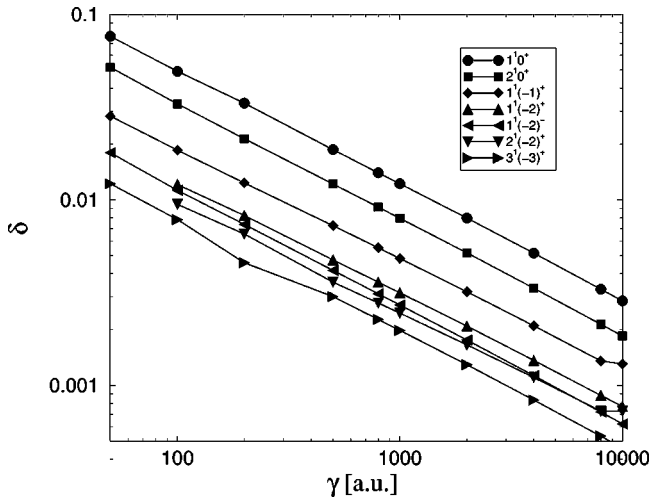


FIG. 2. The parameter  $\delta$  as a function of the field strength for singlet states of various symmetries. It accounts for the state dependent normal finite mass corrections due to the Coulomb interaction.

For the states and field strengths investigated in the present work, we will see that  $\delta(\gamma) \ll 1$ . Therefore,  $\delta$  represents a small correction. Since this correction is due to the Coulomb interaction it is state dependent. In Fig. 2 the quantity  $\delta$  is shown as a function of the magnetic-field strength  $\gamma$  for a few selected singlet states belonging to different symmetries. It can be seen that  $\delta(\gamma)$ , for all states considered, follows a power law  $\delta(\gamma) = C\gamma^{-\lambda}$  with a nearly state independent exponent  $\lambda \approx 0.62$ . The corresponding proportionality constant  $C$  varies over nearly one order of magnitude for the different states.

To understand more of the behavior of the quantity  $\delta$ , we expand the first term on the right-hand side of Eq. (3.1) in powers of  $1/M_0$ . Omitting the spin part, we obtain

$$\mu E\left(\infty, \frac{\gamma}{\mu^2}\right) = E_{\text{rm}}(\gamma) + \frac{\gamma M}{M_0} = \mu \left\{ E(\infty, \gamma) + \frac{2\gamma E'(\infty, \gamma)}{M_0} + O\left(\frac{1}{M_0^2}\right) \right\} \quad (3.5)$$

$$\approx E(\infty, \gamma) - \frac{E(\infty, \gamma)}{M_0} + 2\gamma \frac{E'(\infty, \gamma)}{M_0}. \quad (3.6)$$

Here, the prime indicates the derivative with respect to the field strength. Now  $\Delta E_{\text{rm}}$  and consequently  $\delta$  can be expressed in terms of the eigenenergies of  $H(\infty, \gamma)$

$$\delta \approx \frac{-E(\infty, \gamma) + 2\gamma E'(\infty, \gamma) + \gamma|M|}{\gamma(1+|M|)} - 1. \quad (3.7)$$

The state dependence of  $\delta$  can now be understood as the dependence on the derivative of the eigenenergies  $E(\infty, \gamma)$  with respect to the field strength. We emphasize that the quantities  $E(\infty, \gamma)$  and  $\gamma E'(\infty, \gamma)$  in Eq. (3.7) are almost equal and, therefore, approximately cancel in the superstrong field regime. Thus,  $\delta(\gamma)$  can be approximated by  $\delta(\gamma) \approx \{[E'(\infty, \gamma) + |M|]/(1+|M|)\} - 1$ .

Figure 3(a) illustrates the mass polarization energies  $|E_{\text{mp}}| = |E(M_0, \gamma) - E_{\text{rm}}(\gamma)|$  for the energetically lowest singlet states and Fig. 3(b) for the corresponding triplet states. Here,  $E(M_0, \gamma)$  denotes the eigenenergies of  $H(M_0, \gamma)$ . First, we observe that the absolute values of  $E_{\text{mp}}$  are very small: For  $\gamma = 10^4$  they are at least eight orders of magnitude smaller than the corresponding total energies. They are also small compared to the normal finite mass corrections  $\Delta E_{\text{rm}}$ . For  $\gamma = 10^4$  a.u.  $E_{\text{mp}}$  is typically at least four orders of magnitude smaller than the corresponding normal finite mass corrections. Opposite to the quantity  $\Delta E_{\text{rm}}$  the behavior of  $|E_{\text{mp}}|$  depends strongly on the state. For the states  $1^1 0^+, 1^1 (-1)^+, 1^1 (-2)^+, 1^1 (-3)^+$  the quantity  $|E_{\text{mp}}|$  increases with increasing field strength. These states contain so-called mag-

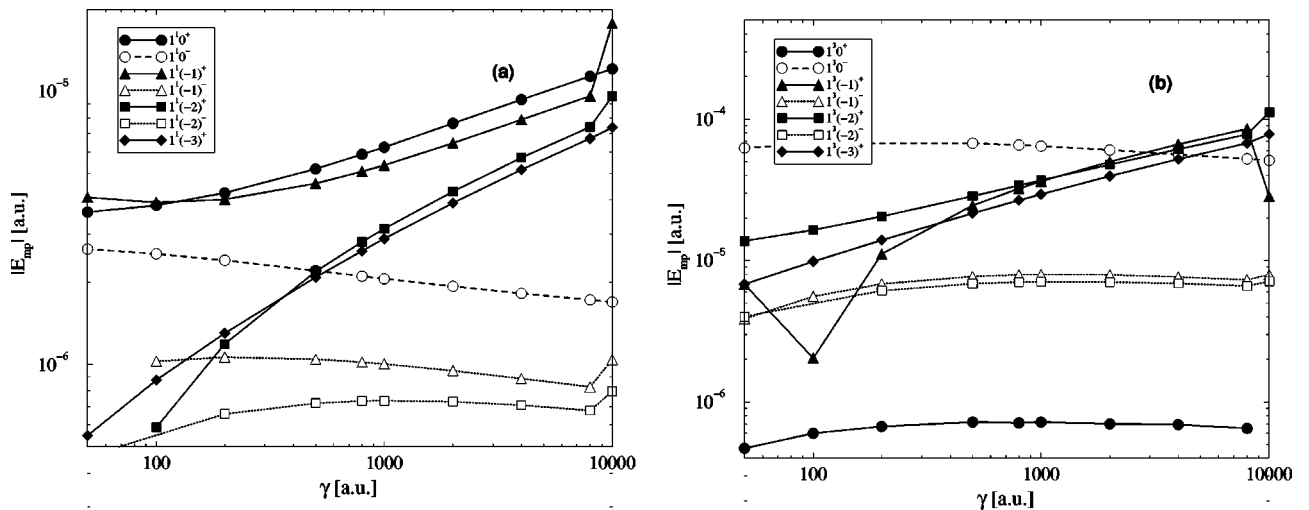


FIG. 3. The absolute values of the mass polarization energies  $|E_{\text{mp}}| = |E(M_0, \gamma) - E_{\text{rm}}(\gamma)|$  for selected singlet (a) and triplet (b) states as a function of the magnetic-field strength  $\gamma$ .

netically tightly bound orbitals ( $1s_0, 2p_{-1}, 3d_{-2}, \dots$ ), which are defined in the infinite nuclear mass frame [6,44,45] and possess a logarithmically diverging binding energy for  $\gamma \rightarrow \infty$ . An increase of  $|E_{\text{mp}}|$  can also be observed in Fig. 3(b) for the states  $1^3(-1)^+, 1^3(-2)^+,$  and  $1^3(-3)^+$ , which contain also magnetically tightly bound orbitals. For the states  $1^{2S+1}0^-, 1^{2S+1}(-1)^-$  as well for  $1^30^+|E_{\text{mp}}|$  remains almost constant as a function of the magnetic-field strength. This effect can be easily understood: For the magnetically tightly bound states the electrons are close to each other in a relatively narrow region of space and therefore electron correlation is important. On the other hand, the mass polarization operator is sensitive to electronic correlation, due to the fact that it contains products of operators of both electrons. The sign of  $E_{\text{mp}}$  is not shown in Fig. 3. It is positive for states containing tightly bound orbitals and negative otherwise. The only exception is the state  $1^30^+$ , which does not belong to the tightly bound states, but nevertheless  $E_{\text{mp}}$  has a positive sign.

#### IV. RESULTS

In the following, we present our results for the ionization energies and transition wavelengths of the helium atom for magnetic fields ranging from 100 a.u. to 10 000 a.u. These investigations have been performed for the magnetic quantum numbers  $M=0, -1, -2, -3$ , singlet and triplet states as well as positive and negative  $z$  parity. Only for  $M=-3$  exclusively states with a positive-positive  $z$  parity have been studied. Typically six excited states of each symmetry are investigated.

##### A. Ionization energies

According to the above, the reader should keep in mind that the exact values for the ionization threshold  $\text{He} \rightarrow \text{He}^+ + e^-$  as a function of  $\gamma$  are unknown. As a consequence, we cannot evaluate the ionization energies accurately. However, the ionization energies calculated by using different approximate threshold energies  $E_{\text{fn}}^{\text{th}}, E_{\text{mc}}^{\text{th}}, E_{\text{zpmc}}^{\text{th}}, E_{\text{ad}}^{\text{th}}$  introduced above show the same trend: the number of bound states of the helium atom becomes finite for superstrong magnetic fields in contrast to the situation without a magnetic field, or in the limit of an infinitely heavy nucleus, where the helium atom possesses an infinite number of bound states. Only the so-called magnetically tightly bound states remain bound for the complete regime of field strengths investigated in the present work. We consider in the following the quantity  $E_{\text{ion}} = E_{\text{zpmc}}^{\text{th}} - E(M_0, \gamma)$  as a function of the field strength together with the above mentioned approximations for the threshold energy.

Figure 4(a) shows  $E_{\text{ion}}$  for the six energetically lowest states of zero magnetic quantum number and positive  $z$  parity. The  $1^10^+$  state is the most tightly bound state. In strong magnetic fields it represents, however, not the ground state of the atom, because energetically low-lying states are fully spin polarized in the high-field regime. The ground state is given by the  $1^3(-1)^+$  state, which is also a tightly bound state. Figure 4(a) shows, that  $E_{\text{ion}}$  increases for the state

$1^10^+$ , but remains approximately constant for all other states as a function of the magnetic-field strength. Furthermore, we observe that all states  $\nu^10^+$  with  $\nu > 1$  as well as the corresponding triplet states pass the ionization threshold energies being either  $E_{\text{ad}}^{\text{th}}$  or  $E_{\text{mc}}^{\text{th}}$  with increasing field strength. The only remaining bound state for  $\gamma = 10^4$  a.u. is the  $1^10^+$  state.

We present in Figure 4(b)  $E_{\text{ion}}(\gamma)$  for states with  $M^{\Pi_z} = 0^-$ . For these states  $E_{\text{ion}}(\gamma)$  varies only to a very minor extent, which is due to the fact, that none of these states is a tightly bound one, and none of these states remains bound when  $\gamma$  approaches  $10^4$  a.u. For the triplet states with negative  $z$  parity the quantity  $E_{\text{ion}}$  decreases slightly for  $\gamma > 100$  a.u. This is not due to the finite mass effect, but can be also observed for the quantity  $E_{\text{fn}}^{\text{th}} - E(\infty, \gamma)$ , whereas this quantity increases monotonically for all other states investigated in the present work. The reason is the complicated interplay between correlation, which tends to increase ionization energies and Coulomb repulsion, which tends to decrease it. For the states with  $M=0$  the electrons are confined in a very small domain of space, which increases correlation as well as the Coulomb repulsion. On the other hand, for the triplet states the electrons are separated, because the wave function is antisymmetric, which reduces both effects. For the  $\nu^30^-$  states the increase of the correlation energy is smaller than the increase of the Coulomb repulsion energy.

In Fig. 4(c)  $E_{\text{ion}}(\gamma)$  is shown for the states  $\nu^{2S+1}(-1)^+$ . For the magnetically tightly bound states  $1^1(-1)^+$  and  $1^3(-1)^+$  the ionization energy remains positive, i.e., these states are bound in the complete regime  $\gamma < 10^4$  a.u. For higher excited states, i.e.,  $\nu^{2S+1}(-1)^+$  with  $\nu > 1$  the energy  $E(M_0, \gamma)$  becomes even larger than  $E_{\text{zpmc}}^{\text{th}}$  and, therefore,  $E_{\text{ion}}$  decreases strongly on the logarithmic scale. To understand this, we review Eq. (3.1): The dominant term on the right-hand side is of the form  $-M\gamma/M_0$  (the spin part does not affect the ionization energies). Therefore,  $E(M_0, \gamma)$  for states with  $M < 0$  raises by approximately this amount and will pass the threshold at lower-field strength than their counterparts with  $M=0$ .

Figure 4(d) shows our results  $E_{\text{ion}}(\gamma)$  for  $M^{\Pi_z} = -1^-$ . A similar behavior as for the energies of the states  $\nu^{2S+1}(-1)^+$ , with  $\nu > 1$  in Fig. 4(c) is observed: The ionization energy as a function of the field strength decreases rapidly for all states. This is due to the fact, as mentioned above, that the finite mass corrections force these states to pass even the  $E_{\text{zpmc}}^{\text{th}}$  threshold and consequently, they become unbound.

In Fig. 5(a), we present our results for  $E_{\text{ion}}$  for the energetically lowest singlet and triplet states with  $M=-2$  and positive  $z$  parity. Similar to Fig. 4(c) the quantity  $E_{\text{ion}}$  rises for the two energetically lowest singlet and triplet states from 1.8 a.u. to  $\approx 10$  a.u. These two states belong to the magnetically tightly bound ones. In contrast to the  $2^{2S+1}(-1)^+$  states in Fig. 4(a),  $E_{\text{ion}}$  for the state  $2^1(-2)^+$ , which is the first-excited singlet state of this symmetry, does also rise and stays bound within the complete regime of field strength considered here. This is a remarkable feature since the influence of the finite mass effects for this state is even more pronounced than for the states with  $M=-1$ . The reason for this behavior is the presence of an avoided crossing which occurs

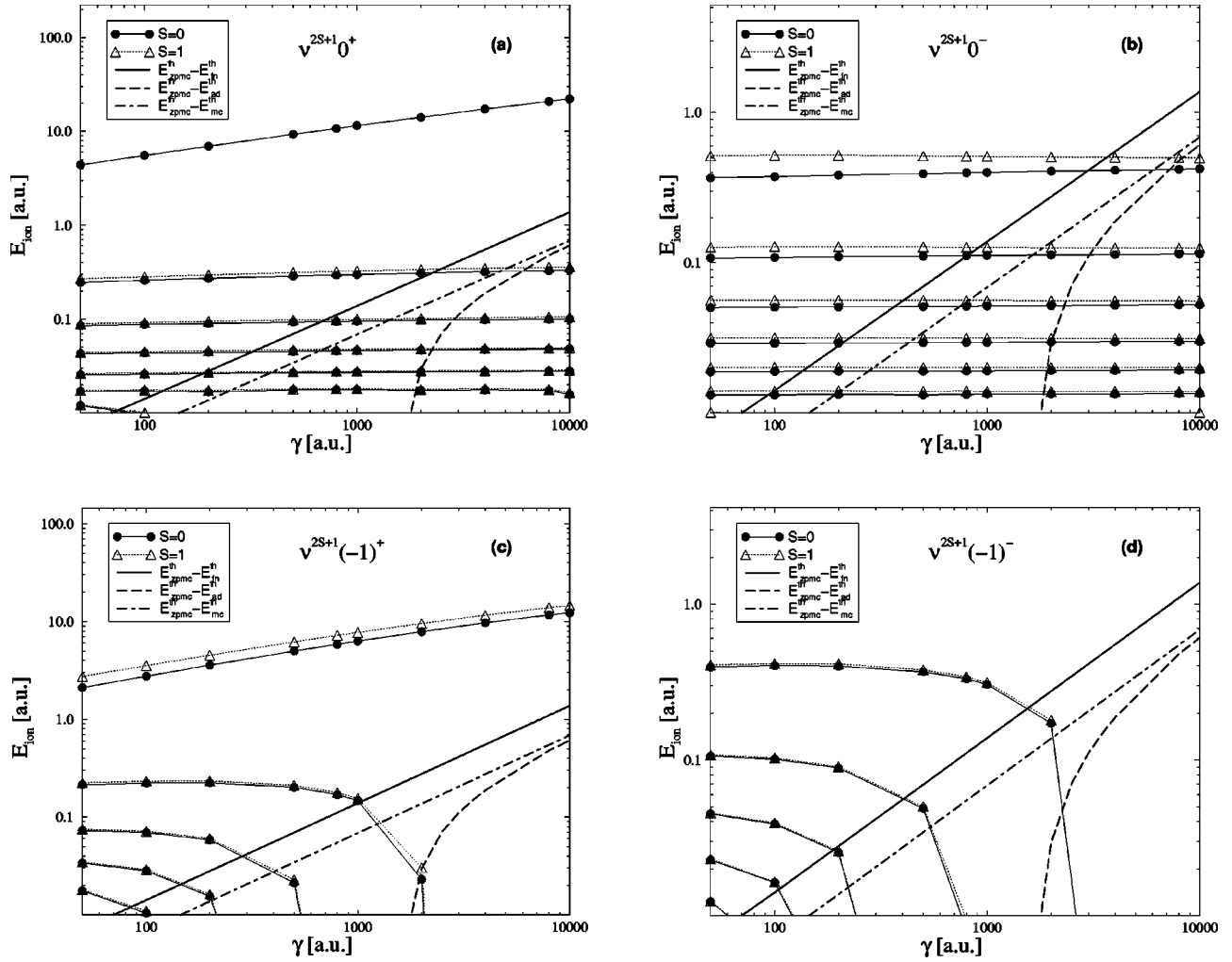


FIG. 4. Ionization energies  $E_{\text{ion}} = E_{z\text{pmc}}^{\text{th}} - E(M_0, \gamma)$  of the helium atom for the  $\nu^{2S+1}M^{\Pi_z}$  states ( $\nu = 1, 2, \dots$ , numbered from top to bottom). Note that the threshold  $E_{z\text{pmc}}^{\text{th}}$  overestimates the ionization energies. Different approximations to the exact threshold such as  $E_{\text{mc}}^{\text{th}}$ ,  $E_{\text{ad}}^{\text{th}}$ , and the fixed nucleus ionization threshold  $E_{\text{fn}}^{\text{th}}$  are given as a difference to  $E_{z\text{pmc}}^{\text{th}}$ . (a)  $E_{\text{ion}}$  for  $M^{\Pi_z} = 0^+$ , (b)  $E_{\text{ion}}$  for  $M^{\Pi_z} = 0^-$ , (c)  $E_{\text{ion}}$  for  $M^{\Pi_z} = -1^+$ , (d)  $E_{\text{ion}}$  for  $M^{\Pi_z} = -1^-$ .

at  $\gamma \approx 100$  a.u. It can be seen that  $E_{\text{ion}}$  for the higher excited singlet states are raised as well and approach the corresponding values for the next energetically higher triplet states.

The ionization energies for the negative  $z$  parity states for  $M = -2$  in Fig. 5(b) look similar to those for  $M = -1$  in Fig. 4(d). All states of this symmetry become unbound with increasing field strength. As mentioned above the influence of the finite nuclear mass increases with increasing magnetic quantum number  $|M|$ , therefore, the states  $\nu^{2S+1}(-2)^-$  become unbound at lower-field strengths than the corresponding states with  $M = -1$ .

In Fig. 5(c), we observe that  $E_{\text{ion}}$  of the energetically lowest singlet and triplet states with  $M^{\Pi_z} = -3^+$  is positive for all field strengths, considered in the present work. These two states belong to the magnetically tightly bound states and they remain bound within the complete regime of field strengths considered here. Similar to Fig. 5(a) avoided crossings take place around  $\gamma \approx 200$  a.u. This can hardly be seen in Fig. 5(c) but becomes much more evident by inspecting the quantity  $E_{\text{fn}}^{\text{th}} - E(\infty, \gamma)$ . But unlike the spectrum of  $M^{\Pi_z}$

$= -2^+$ , where  $E_{\text{ion}}$  for the first excited *singlet* state is raised, here  $E_{\text{ion}}$  for the *triplet* state  $2^3(-3)^+$  is raised and remains, therefore, bound for relatively high-field strengths. Nevertheless, the energy of the state  $2^3(-3)^+$  passes the ionization threshold for  $\gamma$  approaching  $10^4$  a.u. and, therefore, becomes unbound due to the influence of the finite nuclear mass effects.

## B. Transition wavelengths

In contrast to the ionization energies the transition wavelengths can be calculated from our total energies without the knowledge of accurate energy thresholds. The property which remains undetermined for the transition wavelengths is the exact field strength, for which the particular bound-bound transition disappears, i.e., the field strength for which one of the involved bound states enters the continuum. Therefore, we refer the total energy of a state to the threshold  $E_{z\text{pmc}}^{\text{th}}$  in order to decide upon its bound character as a function of the field strength. According to the discussion pro-

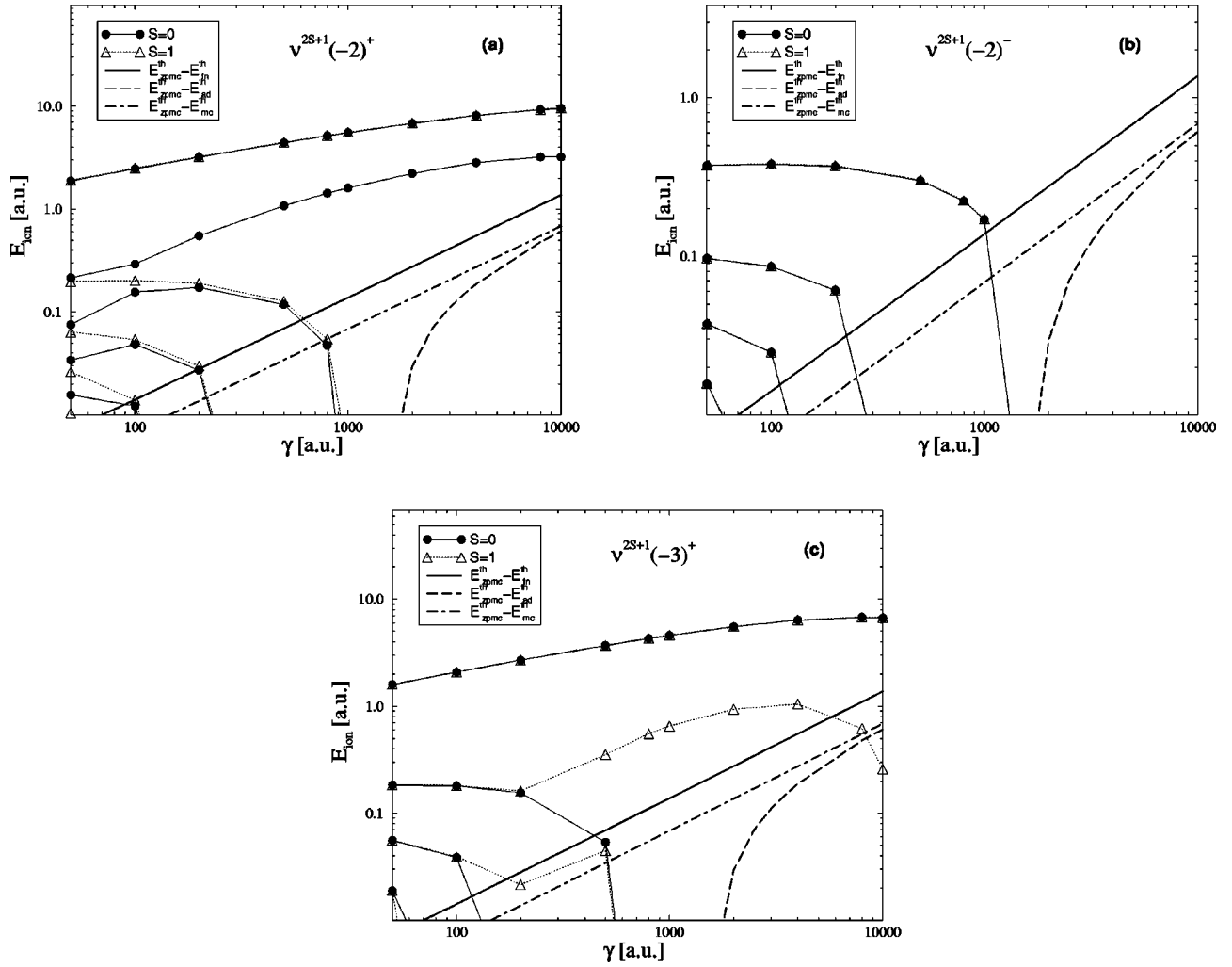


FIG. 5. Ionization energies  $E_{\text{ion}}$  of the helium atom for the electronic states  $\nu^{2S+1}M^{\Pi_z}$  with  $M = -2$  and  $M = -3$  as a function of the magnetic-field strength  $\gamma$ . (a)  $E_{\text{ion}}$  for  $M^{\Pi_z} = -2^+$ , (b)  $E_{\text{ion}}$  for  $M^{\Pi_z} = -2^-$ , (c)  $E_{\text{ion}}$  for  $M^{\Pi_z} = -3^+$ .

vided in Sec. II C the true field strength for which the state becomes unbound is lower than the value obtained by referring the total energies to  $E_{\text{zpmc}}^{\text{th}}$ .

Figures 6(a)–6(c) show the spectra of the linearly polarized transitions  $\nu^{2S+1}M^+ \rightarrow \mu^{2S+1}M^-$  for  $M = 0, -1, -2$ , respectively.  $\nu$  and  $\mu$  range from 1 to 5 for each part. Linearly polarized transitions show the general feature of two well-separated parts of their spectrum. One part consists of small transition wavelengths  $\lambda(\gamma)$  below 400 Å that decrease with a power law for increasing field strength. The corresponding transitions generically involve magnetically tightly bound states. In case of Figs. 6(a)–6(c) these are the  $1^1 0^+$ ,  $1^{2S+1}(-1)^+$ , and  $1^{2S+1}(-2)^+$  states, respectively. Above 1000 Å, we encounter the long wavelength part of the spectrum, which involves transitions among higher excited states ( $\nu, \mu > 1$ ). These transitions are rather insensitive to the field, i.e., the transition wavelengths remain approximately constant with increasing field strength. These general features for the linearly polarized transitions can be clearly seen in Figs. 6(a) and 6(b). Figure 6(c) shows, to some extent, deviations from this behavior.

As discussed in Sec. IV A the states  $\nu^1(-2)^+$  with  $\nu > 1$  undergo an avoided crossing which severely changes its energy as a function of the field strength, compared to the states  $\mu^1(-2)^-$ . Therefore, the singlet transitions shown in Fig. 6(c), which involve  $\nu^1(-2)^+$  and  $\nu > 1$  show a more prominent field dependence, compared to the other excited linearly polarized transitions. Particularly, we draw the attention of the reader to the wavelengths of the transitions  $2^1(-2)^+ \rightarrow \nu^1(-2)^-$ , which are shown as dotted curves, and those of  $3^1(-2)^+ \rightarrow \nu^1(-2)^+$ , which are shown as dashed curves. The reader should also note the different scales of field strengths in Fig. 6(a) compared to Figs. 6(b) and 6(c). The latter are due to finite nuclear mass effects, which causes the corresponding bound states to enter the continuum.

Figures 7(a)–7(e) show the wavelengths for the circularly polarized transitions  $\nu^{2S+1}M^{\Pi_z} \rightarrow \mu^{2S+1}(M-1)^{\Pi_z}$  for ( $M = 0, \Pi_z = \pm 1$ ), ( $M = -1, \Pi_z = \pm 1$ ), and ( $M = -2, \Pi_z = +1$ ), respectively. The quantum numbers  $\mu$  and  $\nu$  cover the range 1–5 for each part.

For the circularly polarized transitions only those spectra possess a part with short wavelengths ( $\lambda < 300$  Å) [see Figs.



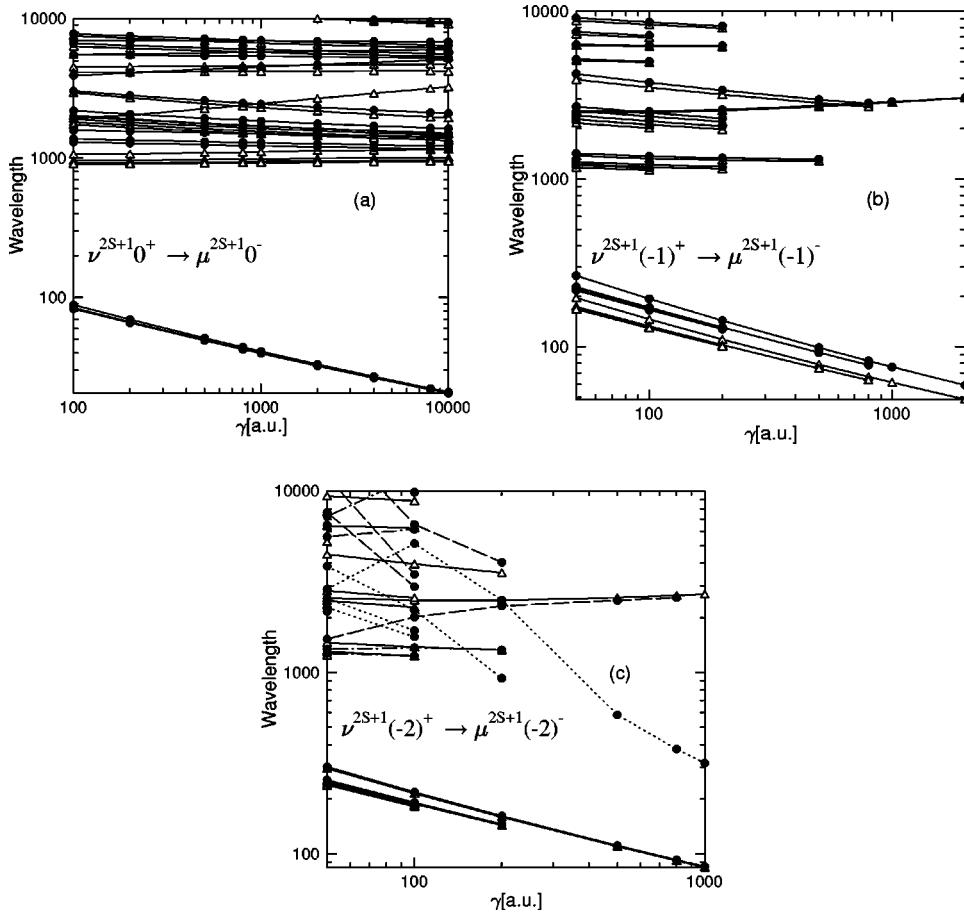


FIG. 6. Wavelengths of linearly polarized transitions of the singlet and triplet states from  $\nu^{2S+1}M^+$  to  $\mu^{2S+1}M^-$  in Ångström as a function of the magnetic-field strength in atomic units.  $\nu$  and  $\mu$  range typically from 1 to 5. Only bound-bound transitions (in the sense defined in the text) with a wavelength below  $10^4$  Å are shown. White circles indicate singlet transitions, black triangles triplet transitions. For a detailed description of part (c) see text. (a)  $M=0$ , (b)  $M=-1$ , (c)  $M=-2$ .

7(a), 7(c), and 7(e)] that involve states with positive  $z$  parity  $\Pi_z$ . This is again due to the tightly bound character of the  $1^1 0^+$ ,  $1^{2S+1}(-1)^+$ ,  $1^{2S+1}(-2)^+$ , and  $1^{2S+1}(-3)^+$  states. The long wavelengths part of the spectra ( $\lambda > 1000$  Å) are, in contrast to the corresponding linearly polarized spectra, strongly dependent on the field strength. This effect is caused by the normal finite mass corrections, which are more pronounced for the states with the higher absolute value of the magnetic quantum number [see Eq. (3.4) and discussion in Sec. III].

Deviations from the general pattern, described above can be found in Figs. 7(c) and 7(e). In Fig. 7(c) the singlet and triplet transition, drawn with dashed lines show a particular behavior. These curves correspond to transitions  $1^1(-1)^+ \rightarrow 1^1(-2)^+$  and  $1^3(-1)^+ \rightarrow 1^3(-2)^+$ , respectively. They follow approximately a power law, similar to the transition wavelengths in the short wavelength part. However, the absolute value of their wavelengths is larger by a factor of 2 for the triplet transition, and a factor 4 for the singlet transition. This is due to the less pronounced energetical separation of the tightly bound states  $2^{S+1}(-1)^+$  and  $2^{S+1}(-2)^+$ . A similar feature can be found in Fig. 7(e) belonging to the transitions  $1^{2S+1}(-2)^+ \rightarrow 1^{2S+1}(-3)^+$  (dashed line). But here singlet and triplet transition wavelengths are almost equal.

The curves drawn with dotted lines in Fig. 7(c) correspond to transitions  $\nu^1(-1)^+ \rightarrow 2^1(-2)^+$  ( $\nu > 1$ ). The wavelengths for these transitions decrease strongly with in-

creasing field strength, due to the above mentioned avoided crossing of the  $2^1(-2)^+$  state. The singlet transitions  $2^1(-2)^+ \rightarrow \nu^1(-3)^+$  ( $\nu > 1$ ) shown in Fig. 7(e) as dotted curves behave similar. Particularly, we want to mention the transition  $1^1(-2)^+ \rightarrow 2^1(-3)^+$  [dashed dotted line in Fig. 7(e)], because the avoided crossing results in a wavelength which is almost constant as a function of the magnetic-field strength.

## V. BRIEF SUMMARY

We have presented the first systematic full CI calculations for helium in superstrong magnetic fields, taking into account the effects of finite nuclear mass. These effects are extremely important in the superstrong field regime, because the relevant parameter for the finite nuclear mass effects is  $\gamma/M_0$ . We analyzed the influence of the normal and the specific finite nuclear mass effects. It has been shown that the leading finite nuclear mass effect does not depend on the specific state, but only on the magnetic quantum number. The state dependent part of the normal finite mass effects is related to the derivative of the total energy of the corresponding state with respect to the magnetic-field strength in the infinite nuclear mass frame. Furthermore, it has been shown that the specific mass effects, which are caused by the mass polarization operators, are very small compared to the total energies and small compared to the leading normal mass effects  $\Delta E_{\text{fm}}^e$ .

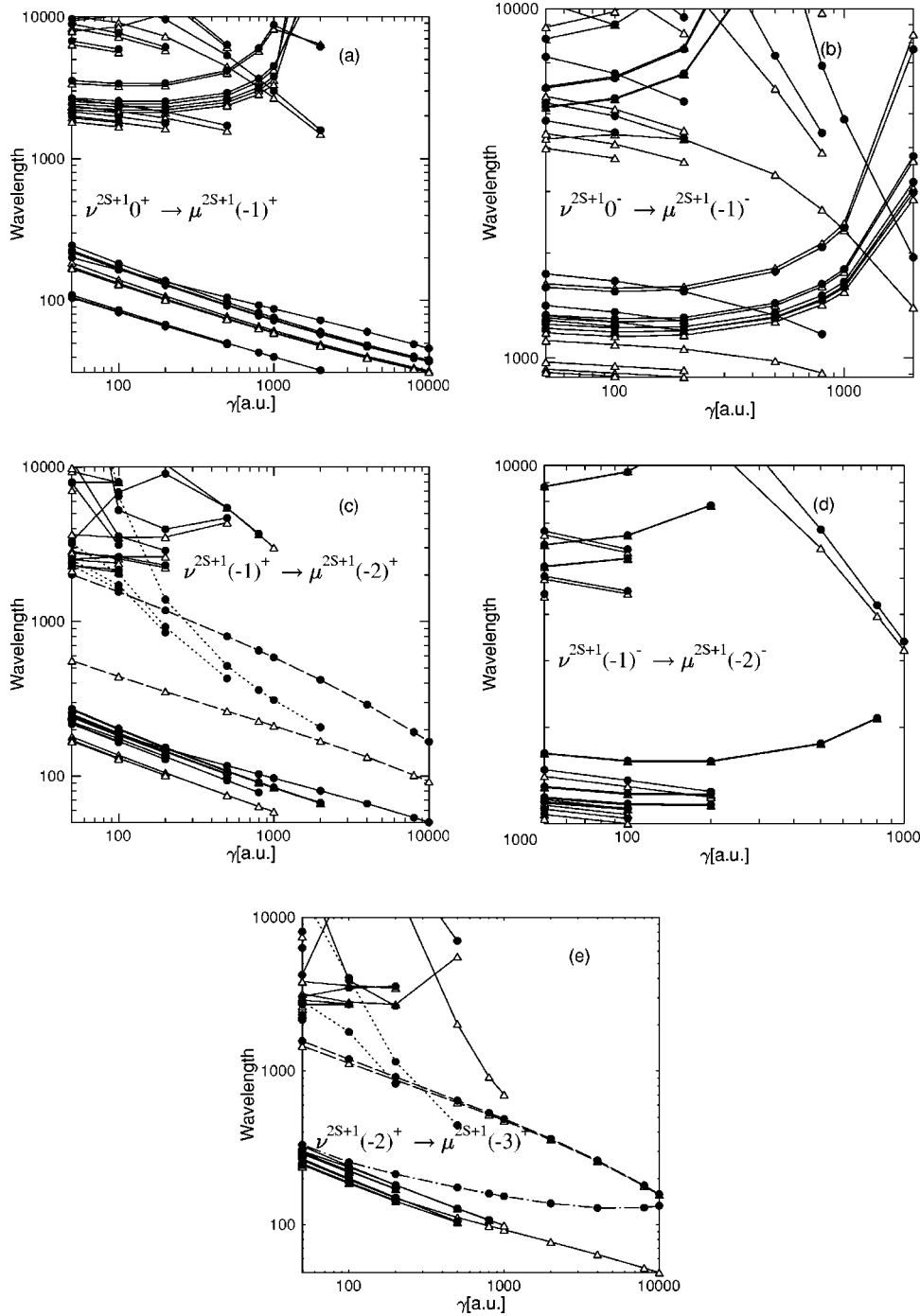


FIG. 7. Wavelengths of circularly polarized transitions between the singlet and triplet states  $\nu^{2S+1}M^{\Pi_z}$  and  $\mu^{2S+1}(M-1)^{\Pi_z}$  in Angstrom as a function of the magnetic-field strength in atomic units.  $\nu$  and  $\mu$  range typically from 1 to 5. Only bound-bound transitions (in the sense defined in the text) with a wavelength below  $10^4 \text{ \AA}$  are shown. Black circles indicate singlet transitions, whereas white triangles indicate transitions between triplet states. For a detailed description of part (c) and (e) see text. (a)  $M=0, \Pi_z=+$  (b)  $M=0, \Pi_z=-$ , (c)  $M=-1, \Pi_z=+$ , (d)  $M=-1, \Pi_z=-$ , (e)  $M=-2, \Pi_z=+$ .

In the superstrong magnetic-field regime, the spectrum of helium is terminated by the effects of the finite nuclear mass. We found that only a comparatively small number of states is bound in the complete regime of magnetic-field strengths investigated in the present work. Although the exact ionization threshold for helium is unknown, all available approximations to the exact threshold confirm this trend. Transition wavelengths for many linear and circularly polarized transitions were provided. Their typical behavior has been identified and the effects of the finite mass on the transition wavelengths has been analyzed.

An accurate calculation of the critical-field strengths (i.e., the field strengths where the individual states become unbound), as well as the ionization energies, requires a detailed investigation of the ground state of the moving helium positive ion in a magnetic field.

#### ACKNOWLEDGMENTS

The Deutsche Forschungsgemeinschaft (O.A.A.) is gratefully acknowledged for financial support. We thank D. Wickramasinghe for valuable discussions.

- [1] J. Angel, J. Liebert, and H.S. Stockmann, *Astrophys. J.* **292**, 260 (1985).
- [2] J. Angel, *Annu. Rev. Astron. Astrophys.* **16**, 487 (1978).
- [3] J.L. Greenstein, R. Henry, and R.F. O'Connell, *Astrophys. J.* **289**, L25 (1985).
- [4] G. Wunner, W. Rösner, H. Herold, and H. Ruder, *Astron. Astrophys.* **149**, 102 (1985).
- [5] D.T. Wickramasinghe and L. Ferrario, *Astrophys. J.* **327**, 222 (1988).
- [6] H. Ruder, G. Wunner, H. Herold, and F. Geyer, *Atoms in Strong Magnetic Fields* (Springer-Verlag, Berlin, 1994).
- [7] Y.P. Kravchenko, M.A. Liberman, and B. Johansson, *Phys. Rev. A* **54**, 287 (1996).
- [8] S. Jordan, P. Schmelcher, W. Becken, and W. Schweizer, *Astron. Astrophys. Lett.* **336**, L33 (1998).
- [9] S. Jordan, P. Schmelcher, and W. Becken, *Astron. Astrophys.* **376**, 614 (2001).
- [10] D.T. Wickramasinghe and L. Ferrario, *Publ. Astron. Soc. Pac.* **112**, 873 (2000).
- [11] R.O. Mueller, A. Rau, and L. Spruch, *Phys. Rev. A* **11**, 789 (1975).
- [12] J. Virtamo, *J. Phys. B* **9**, 751 (1976).
- [13] P. Pröschl, W. Rösner, G. Wunner, and H. Herold, *J. Phys. B* **15**, 1959 (1982).
- [14] M. Vincke and D. Baye, *J. Phys. B* **22**, 2089 (1989).
- [15] G. Thurner *et al.*, *J. Phys. B* **26**, 4719 (1993).
- [16] W. Becken, P. Schmelcher, and F. Diakonov, *J. Phys. B* **32**, 1557 (1999).
- [17] W. Becken and P. Schmelcher, *J. Phys. B* **33**, 545 (2000).
- [18] W. Becken and P. Schmelcher, *Phys. Rev. A* **63**, 053412 (2001).
- [19] W. Becken and P. Schmelcher, *Phys. Rev. A* **65**, 033416 (2002).
- [20] G.G. Pavlov and A.Y. Potekhin, *Astrophys. J.* **450**, 883 (1995).
- [21] G. G. Pavlov, Y. A. Shibano, V. E. Zavlin, and R. D. Meyer, in *The Lives of Neutron Stars*, Vol 450 of *NATO Advanced Studies Institute, Series C: Mathematical and Physical Sciences*, edited by M. A. Alpar, U. Kiziloğlu, and J. van Paradijs (Kluwer, Dordrecht, 1995), pp. 71–90.
- [22] J.H. Taylor, R.N. Manchester, and A.G. Lyne, *Astrophys. J., Suppl. Ser.* **88**, 529 (1993).
- [23] P. Schmelcher, L. S. Cederbaum, and U. Kappes, in *Conceptual Trends in Quantum Chemistry*, edited by E. S. Kryachko and J. L. Calais (Kluwer, Dordrecht, 1994), pp. 1–51.
- [24] B.R. Johnson, J.O. Hirschfelder, and K.H. Yang, *Rev. Mod. Phys.* **55**, 109 (1983).
- [25] D. Baye, *J. Phys. B* **15**, L795 (1982).
- [26] D. Baye and M. Vincke, *J. Phys. B* **19**, 4051 (1986).
- [27] M. Vincke and D. Baye, *J. Phys. B* **21**, 1407 (1988).
- [28] M. Vincke, *J. Phys. B* **23**, 1991 (1990).
- [29] D. Baye and M. Vincke, *J. Phys. B* **23**, 2467 (1990).
- [30] P. Schmelcher and L. Cederbaum, *Phys. Rev. A* **43**, 287 (1991).
- [31] P. Schmelcher, *Phys. Rev. A* **52**, 130 (1995).
- [32] V.G. Bezchastnov, G.G. Pavlov, and J. Ventura, *Phys. Rev. A* **58**, 180 (1998).
- [33] Z. Chen and S.P. Goldman, *Phys. Rev. A* **45**, 1722 (1992).
- [34] A. Poszwa and A. Rutkowski, *Phys. Rev. A* **63**, 043418 (2001).
- [35] W.E. Lamb, *Phys. Rev. A* **85**, 259 (1959).
- [36] J.E. Avron, I.W. Herbst, and B. Simon, *Ann. Phys. (N.Y.)* **114**, 431 (1978).
- [37] V. Pavlov-Verevkin and B.I. Zhilinskii, *Phys. Lett.* **78A**, 244 (1980).
- [38] P. Schmelcher and L.S. Cederbaum, *Phys. Rev. A* **37**, 672 (1988).
- [39] U. Kappes and P. Schmelcher, *Phys. Rev. A* **54**, 1313 (1996); **53**, 3869 (1996); **51**, 4542 (1995).
- [40] T. Detmer, P. Schmelcher, F.K. Diakonov, and L. Cederbaum, *Phys. Rev. A* **56**, 1825 (1997).
- [41] T. Detmer, P. Schmelcher, and L. Cederbaum, *Phys. Rev. A* **57**, 1767 (1998); **61**, 043411 (2000); **64**, 023410 (2001); *J. Chem. Phys.* **109**, (1998); *J. Phys. B* **28**, (1995).
- [42] O.-A. Al-Hujaj and P. Schmelcher, *Phys. Rev. A* **61**, 063413 (2000).
- [43] W. Becken and P. Schmelcher, *J. Comput. Appl. Math.* **126**, 449 (2000).
- [44] R. Loudon, *Am. J. Phys.* **27**, 649 (1959).
- [45] M.V. Ivanov and P. Schmelcher, *Phys. Rev. A* **57**, 3793 (1998); **60**, 3558 (1999); *J. Phys. B* **34**, 2031 (2001); *Eur. Phys. J. D* **14**, 279 (2001).